(1)

ARMY RESEARCH LABORATORY

Fracture Analysis of an All-Ceramic Bearing System

Jeffrey J. Swab and Mary P. Sweeney

ARL-TR-512

September 1994

Sponsored by
Advanced Research Projects Agency (ARPA)
3701 N. Fairfax Drive
Arlington, VA 22203-1714

REPORT DOCUMENTATION PAGE

Form Approved OMB No. 0704-0188

1. AGENCY USE ONLY *(Leave blank)*

2. REPORT DATE
September 1994

3. REPORT TYPE AND DATES COVERED
Final Report

4. TITLE AND SUBTITLE
Fracture Analysis of an All-Ceramic Bearing System

5. FUNDING NUMBERS

6. AUTHOR(S)
Jeffrey J. Swab and Mary P. Sweeney*

7. PERFORMING ORGANIZATION NAME(S) AND ADDRESS(ES)
U.S. Army Research Laboratory
Watertown, MA 02172-0001
ATTN: AMSRL-MA-CA

8. PERFORMING ORGANIZATION REPORT NUMBER
ARL-TR-512

9. SPONSORING/MONITORING AGENCY NAME(S) AND ADDRESS(ES)
Advanced Research Projects Agency (ARPA)
3701 N. Fairfax Drive
Arlington, VA 22203-1714

10. SPONSORING/MONITORING AGENCY REPORT NUMBER

11. SUPPLEMENTARY NOTES
*Missile Systems Division, Raytheon Company, Tewksbury, MA 01876.

12a. DISTRIBUTION/AVAILABILITY STATEMENT
Approved for public release; distribution unlimited.

12b. DISTRIBUTION CODE

13. ABSTRACT *(Maximum 200 words)*

The report summarizes the fracture mechanism of an all-ceramic duplex spin bearing which was tested to failure to establish a design load margin. This bearing is part of a gyro-optics assembly being developed for use in an infrared seeker. The analysis revealed that machining-induced microcracks grew in the inner raceway beneath a ball. These microcracks coalesced to form macrocracks which led to fracture of the inner race and the failure of the bearing system.

14. SUBJECT TERMS
Ceramic bearing, Fractography, Silicon nitride

15. NUMBER OF PAGES
35

16. PRICE CODE

17. SECURITY CLASSIFICATION OF REPORT	18. SECURITY CLASSIFICATION OF THIS PAGE	19. SECURITY CLASSIFICATION OF ABSTRACT	20. LIMITATION OF ABSTRACT
Unclassified	Unclassified	Unclassified	UL

NSN 7540-01-280-5500

Standard Form 298 (Rev 2-89)
Prescribed by ANSI Std Z39-18
298-102

CONTENTS

FIGURES

TABLE

INTRODUCTION

All-ceramic (silicon nitride) spin and gimbal bearings were designed and fabricated for use in a miniature infrared (IR) seeker. Ceramic bearings were used to improve the system load capacity over an all steel bearing design; to eliminate the potential of fretting corrosion and to decrease friction, thus improving system performance. As part of this development program, design margin testing was initiated to determine the maximum load capacity of the spin bearings after a redesign of the spin bearing attachment mechanism. Reported herein are the results of a detailed fractographic analysis performed on one of the tested spin bearings. By identifying the load-limiting failure mechanism of this spin bearing design, future all-ceramic bearing applications can be improved based on information provided by the fracture analysis.

SILICON NITRIDE HISTORY

Silicon nitride has long been recognized as a ceramic with great potential to replace steel bearings in certain applications in the machine tool, aerospace, and biotechnology industry.[1,2] Silicon nitride is attractive for these applications because, when properly fabricated, it possesses the following characteristics:

- Low density
- Low friction coefficients
- High hardness and strength (flexure and compression)
- Excellent corrosion resistance
- Low thermal expansion and conductivity
- Ability to maintain these properties up to $\approx 1000^{\circ}C$

Studies[1,3] have shown that a significant improvement in bearing fatigue life can be achieved when steel balls are replaced with silicon nitride balls. The failure mechanism of the ceramic is as important as improved fatigue life in determining if a ceramic bearing can be used. Unlike most other ceramics which fail catastrophically in rolling contact fatigue tests, silicon nitride has been shown to fail due to spallation, the same failure mechanism as its steel counterpart.[4] Additionally, silicon nitride balls have successfully operated in a lubrication starved environment[5-7] and produced less heat than similar steel bearings.[8]

Presently one of the leading commercial ceramic bearing materials is a hot isostatically pressed (HIPed) silicon nitride (NBD-200). A majority of the early ceramic bearing studies focused on a hot-pressed silicon nitride (NC-132).[1,3-6] Both of these silicon nitrides contain approximately 1 w/o MgO to promote densification. The bearing work in the 1970's and 1980's coincided with the development and evaluation of silicon nitrides, especially NC-132, for other structural applications (i.e., heat engines). As a result it was convenient to conduct bearing studies using NC-132, because this material was readily available, extremely consistent and a wealth of property data was being generated.[9-12]

NBD-200 is a third-generation of NC-132. (NBD-100 is the second-generation material.) As stated previously, this material is HIPed, rather than hot pressed, which eliminates any

anisotropic properties. In addition, the HIPing operation allows for near-net-shape pieces to be produced, thus greatly reducing the amount of machining.

MATERIAL

The ceramic bearing system was made from a Norton Advanced Ceramics, East Grandby, CT (NAC) (formerly CERBEC) silicon nitride, tradename Noralide NBD-200, which contains approximately 1 w/o MgO as a densification aid. The bearing components were fabricated to near-net-shape by hot isostatic pressing. The balls were precision finished by Norton Advanced Ceramics while the races were fabricated into cylindrical blanks by NAC and then machined by Miniature Precision Bearings, Keene, NH (MPB) to final dimension through diamond grinding.

The properties of this silicon nitride, as provided by the manufacturer, are listed below:

Table 1.
Properties of NBD-200

Density	(g/cc)	3.16
Elastic Modulus	(GPa)	320
Poisson's Ratio		0.26
Vickers Hardness (10Kg)	(GPa)	16.6
Room Temperature Strength		
Flexure, Mean - MIL STD 1942	(MPa)	800
Weibull Modulus		9.7
Tensile, Mean, As HIPed	(MPa)	400
Compressive, Bulk	(GPa)	3
Hertz Compressive, Ball on Flat	(GPa)	28
Fracture Toughness,	(MPa*$\sqrt{m}$)	4.1
Thermal Expansion Coef. -170°C to 20°C	(10^{-6}/°C)	.43
20°C to 1000°C		2.9
Thermal Conductivity 100°C	(W/m-K)	29.3
500°C		21.3
1000°C		15.5
Maximum Use Temperature	(°C)	1000

ALL-CERAMIC BEARING APPLICATION

Miniature all-ceramic (NBD-200 silicon nitride) gimbal and spin bearings were developed for a common IR seeker, Figure 1, to be employed in the SPARROW-7P and SM-2 Block III missile systems. The gimbal and spin bearings are part of a gyro-optics assembly (GOA), Figures 2 and 3, which performs as both a free gyro and optics system for the seeker.

The main driving force behind the development of the all-ceramic bearings was to increase bearing load capacity. The original seeker design consisted of steel (440C) gimbal and spin

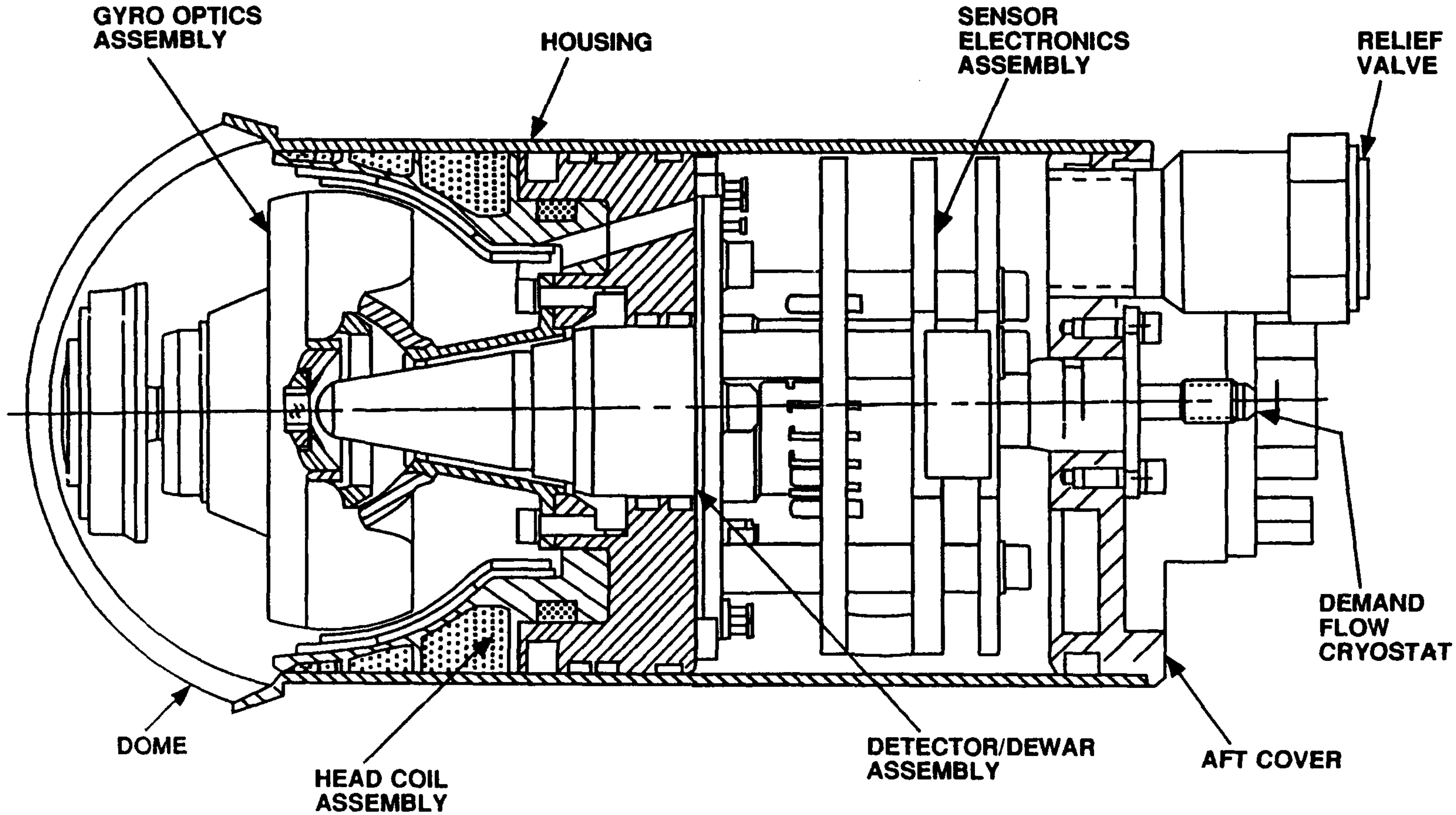

Figure 1. Schematic of the common IR seeker head assembly.

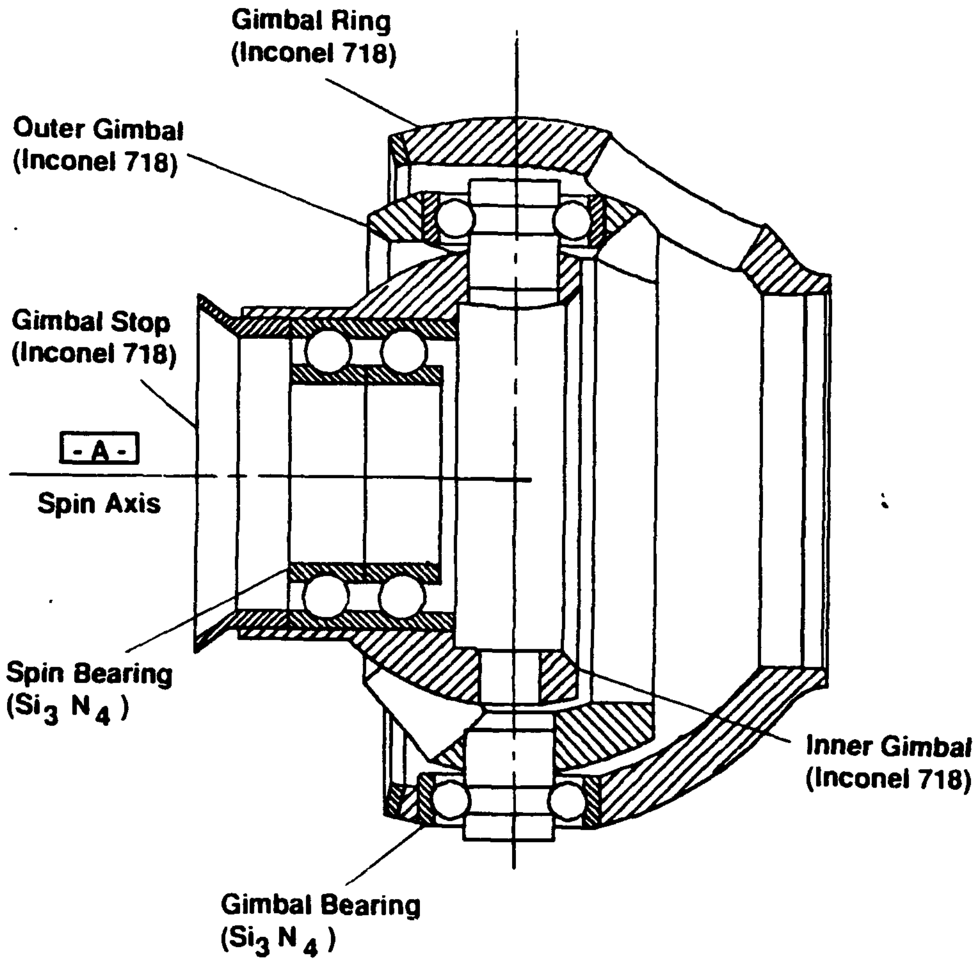

Figure 2. Schematic of the gimbal assembly showing the location of the all-ceramic bearing systems.

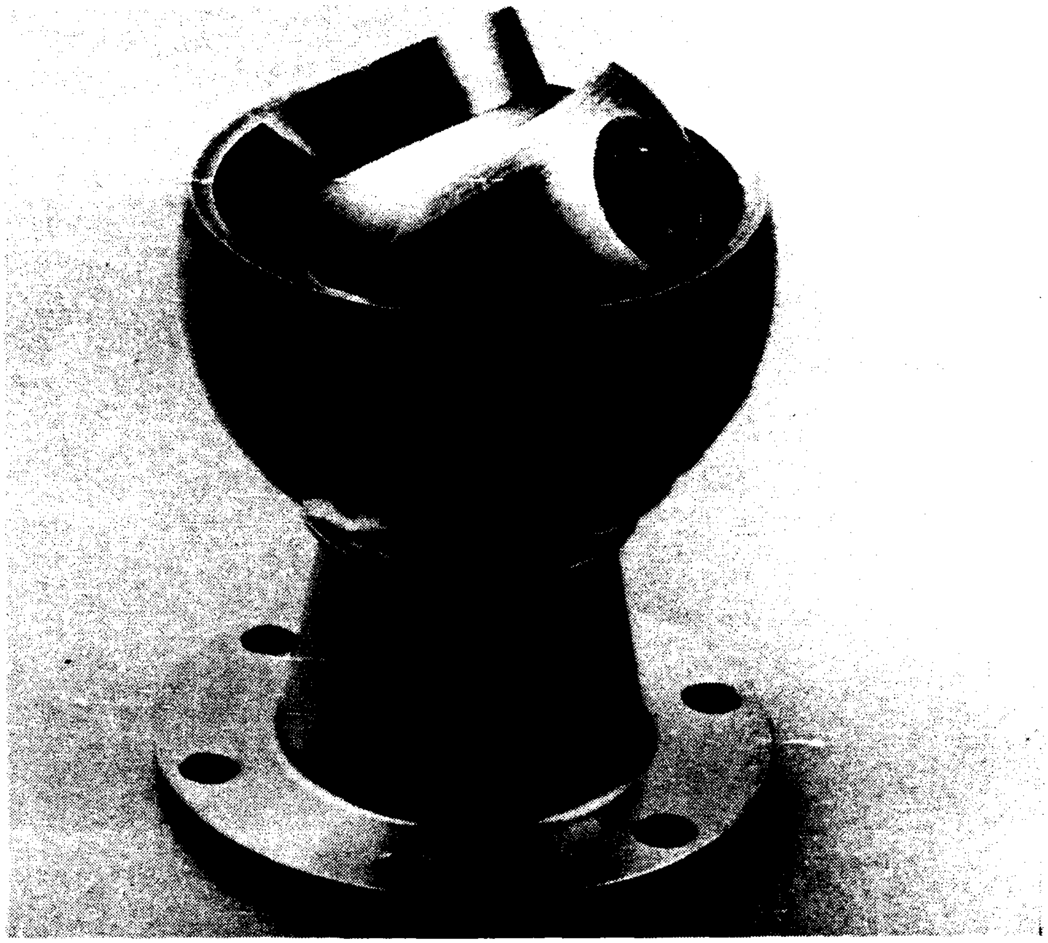

Figure 3. Gimbal assembly containing all-ceramic gimbal and spin bearings.

bearings whose load capacities were marginal for the system requirements. The steel gimbal bearings were full-complement (maximum number of balls in the race) in order to achieve the highest possible load capacity. This full-complement condition, however, increases bearing friction, which degrades the GOA performance.. The all-ceramic gimbal bearings were designed with fewer balls to lower friction yet achieved almost twice the Hertzian load capacity. The basic design of the ceramic spin bearings was similar to that of the steel system. (Hybrid bearings were not considered for this application because they typically have load capacities lower than the all-steel system due to the combination of a "hard" ceramic ball and a "soft" steel raceway.)

Other advantages of the all-ceramic system were the ability to reduce magnetic coupling between the gimbal assembly and the gyro magnet, and effectively eliminate fretting corrosion (microwelding of the ball to the raceway). The latter has been seen to be a problem in other bearing applications were all-steel systems are exposed to long-term vibrations.[13]

BEARING/GOA ASSEMBLY PROCEDURE

The IR seeker GOA, without the mirror magnet and optics, is shown in Figure 3. This assembly consists of two types of ceramic bearings: one duplex spin bearing, with each raceway containing six balls, Figure 4, and four gimbal bearings, each containing six balls, Figure 5. Ball spacing in the spin bearing is maintained by a lubricant-impregnated polyimide retainer. The gimbal bearing balls are caged in a beryllium-copper retainer and a hydrocarbon lubricant is injected. Both bearing lubricant systems were the same as used in the steel bearing systems.

Figure 4. Overall view of an all-ceramic spin bearing.

Figure 5. Overall view of a gimbal bearing.

The ceramic bearings are assembled in the same manner as the steel bearings. All raceway critical dimensions are measured, and ball sizes are selected for each raceway to obtain the correct preload. Starting torque, average running torque, and peak running torque are then measured for each bearing.

In the seeker GOA, both races of the gimbal bearings are bonded in place to their corresponding gimbal components.[14] The spin bearing outer race is attached to the inner gimbal with a flexible adhesive while the inner race is selectively fitted to its mating part. Friction and deflection are measured for both gimbal and spin bearings to insure that they have been installed and preloaded correctly. The optics are then attached and the GOA is installed into a seeker.

TESTING

The design margin tests were initiated to determine the maximum load capacity of the GOA after a redesign of the spin bearing attachment mechanism. Six spin bearings were selected for testing. A pre-test examination was performed using an optical microscope to inspect the outer and inner races of the spin bearings for possible damage. The bearings were then reassembled and built into engineering GOA's simulating actual hardware. The GOA containing the spin bearing referenced in this paper was subjected to system flight vibration profiles at -37^{o}C with a peak response of 85 G's. After this exposure, the vibration input load levels were increased by 3 dB until the GOA failed. Because the GOA was not operating during the test the bearings were not spinning when failure occurred. After failure the GOA was disassembled and a fracture analysis was performed.

RESULTS

Pre-Test Examination

No evidence of damage on the raceways was observed, but some machining striations were found on the surfaces above and below the raceways. It was also noted that one of the chamfers on one of the inner races had not been machined. This information was helpful during the reconstruction of the inner races.

Design Margin Test Results

The engineering GOA containing the spin bearing evaluated herein survived the required system loading vibration levels. The unit failed at a loading of 270 G's peak during exposure to increasing loading levels. This failure load was $\approx$ 40% higher than the system load requirements.

Fracture Analysis Results

<u>Visual Examination</u> - This examination revealed no damage to the outer race or the balls but the inner races fractured into many pieces. Upon reconstruction it was found that several pieces were missing from both inner races; however, this did not hinder the determination of a possible crack initiation site or the direction of crack propagation. Figures 6 and 7 are montages

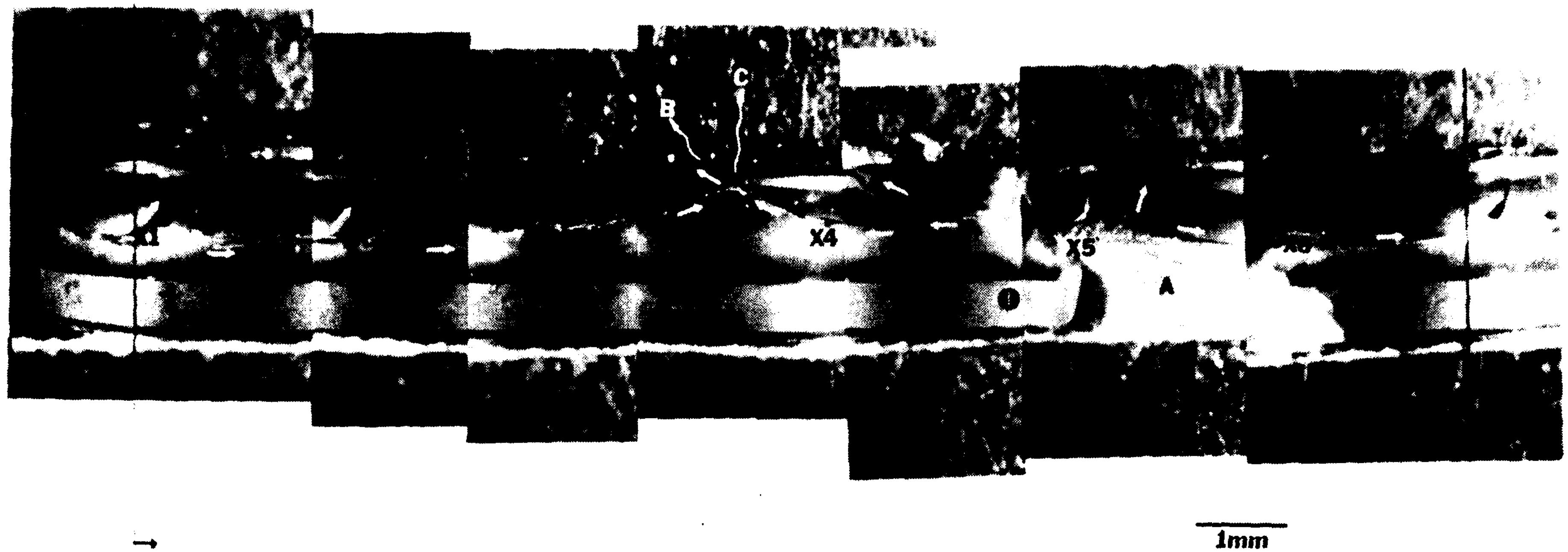

Figure 6. Montage of the reconstructed End #1 inner race. A is a possible area of fracture initiation. B and C are crack termination points. B is were the crack which propagated to the left of area A terminated and C is were the crack which propagated to the right of area A terminated. X indicates the approximate location of each ball. Arrows indicate the direction of crack propagation.

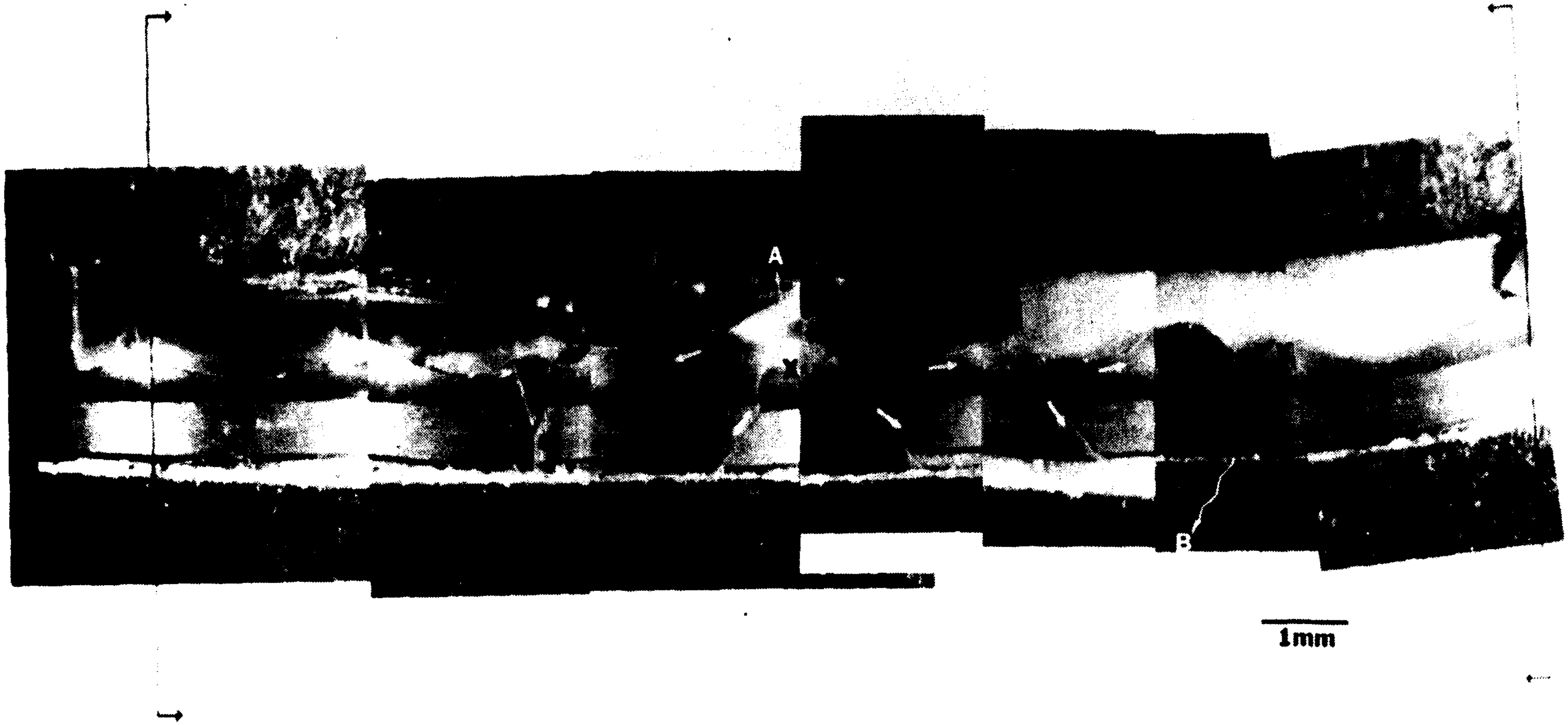

Figure 7. Montage of the reconstructed End #2 inner race. A is a possible area of fracture initiation. B is a crack which was created during reconstruction. X indicates the approximate location of each ball. Arrows indicate possible directions of crack propagation.

of each reconstructed inner race. The race in Figure 6 is labeled as End #1. This is the forward race in the seeker, see Figure 2. The other race, Figure 7, is labeled as End #2.

The reconstruction of End #1 showed that there were two macrocracks which combined to traverse the entire circumference of the raceway. It appears that both macrocracks initiated in the area labeled A with one macrocrack propagating to the left and the other to the right. This is confirmed by inspecting the entire crack propagation pattern and noting the intersection of the cracks at point C. One macrocrack propagated a short distance to the left of area A and was the first to terminate, at the top of the race, (point B). The second macrocrack propagated to the right of area A and traversed the remaining circumference of the raceway and terminated at point C when it encountered the free surface created by the first macrocrack.

Six areas of damage can also be seen in Figure 6. These damage areas coincide with the approximate location of the six balls (marked by the X's in the figure). The amount of damage in these areas appears to diminish as the macrocrack proceeds away from the initiation site.

Reconstructing End #2 was significantly more difficult than End #1 because there were many pieces missing, Figure 7. Even so, there was enough evidence to indicate that, as in End #1, two macrocracks initiated in one location (A) and propagated in opposite directions to traverse the circumference of the raceway. It was beyond the scope of this analysis to determine where the two macrocracks may have intersected. There were areas of damage in End #2, similar to those seen in End #1, which may coincide with the location of the balls, but the correlation was not as clear as in End #1.

<u>Scanning Electron Microscope</u> - Analysis with the Scanning Electron Microscope (SEM) focused on End #1 since most of the pieces were available and there are indications that both inner races fractured in a similar manner.

Three parts, labeled 1, 2 and 3 in Figure 6, of the End #1 inner race were examined. Figures 8 and 9 show the fracture surface of part 1. Both photographs reveal the presence of a series of machining related microcracks which are approximately 25-30 μm deep and connected to the raceway surface. An examination of this fracture surface at an angle, Figure 10, demonstrates that these microcracks have linked together in a step-wise fashion. Characterization of the fracture origin is as follows: Machining Damage, located at the surface with a depth of 25-30 μm, (MS^S, surface, 25-30 μm deep).

The SEM examination of parts 2 (Figure 11 and 12) and 3 (Figure 13) show that the texture of the fracture surface near the location of a ball is very rough but it becomes smoother as the crack proceeds away from this location. The texture will become rough again when the next ball is encountered. The outer edge (raceway) of the fracture surface also is very rough, but the surface texture becomes smoother as the crack proceeds through the raceway cross-section.

Analysis of all surfaces and the characterization of the fracture origin was conducted according to the procedures and guidelines outlined in Military Handbook 790, "Fractography and Characterization of Fracture Origins in Advanced Structural Ceramics".

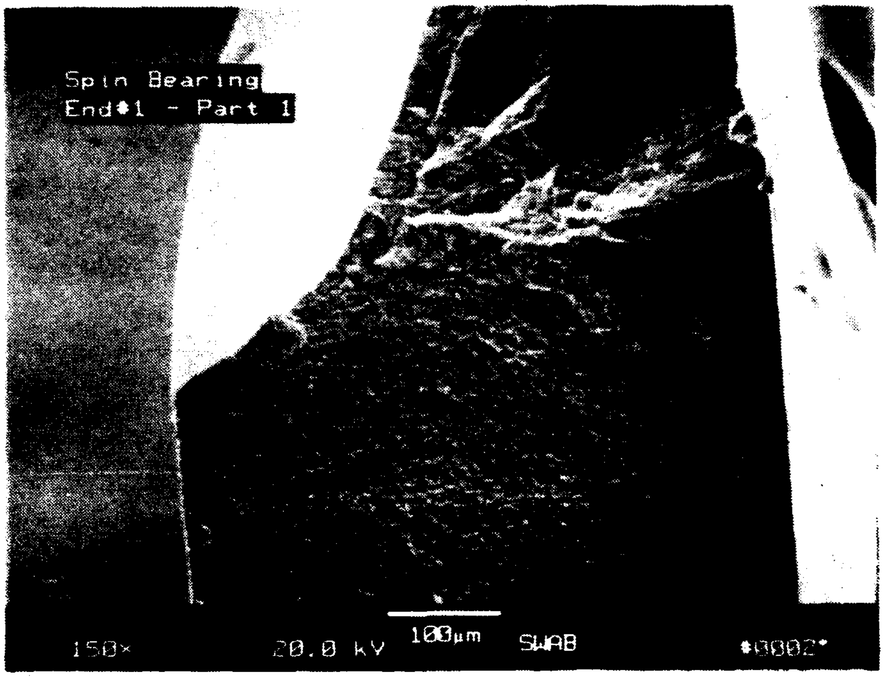

Figure 8. Photograph of the fracture surface of part 1 from End #1.

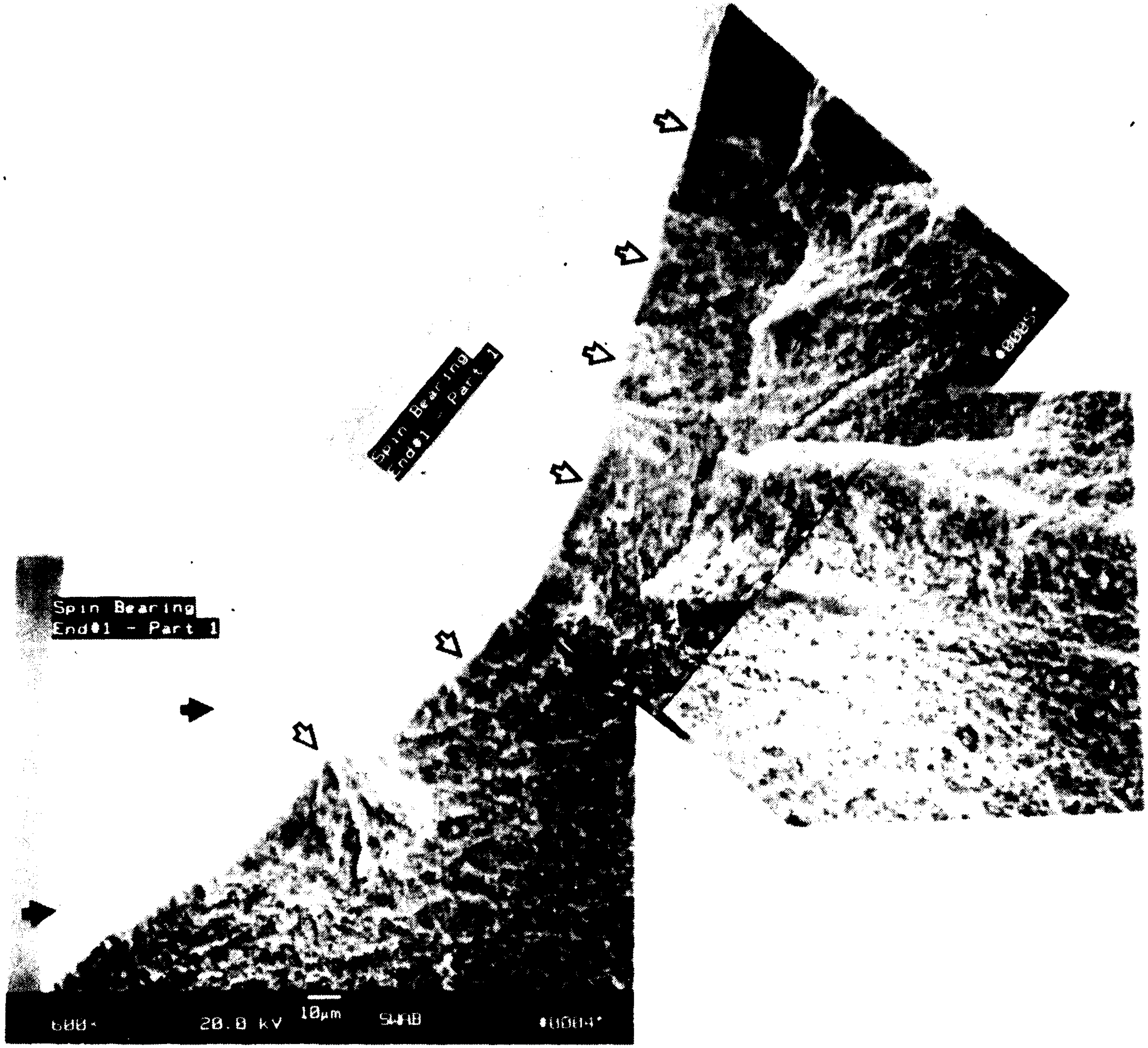

Figure 9. High magnification montage of the fracture surface of part 1 from End #1. Open arrows indicate the surface connected microcracks, (MS^S, surface, 25-30 µm deep). Solid arrows point out some of the machining striations in the raceway.

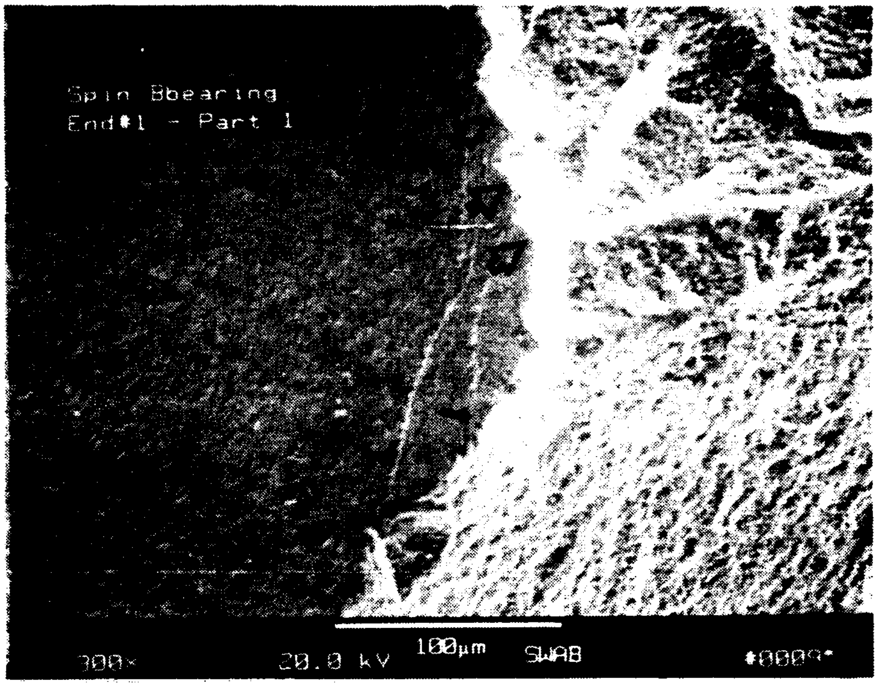

Figure 10. Photograph of the fracture surface of part 1 from End #1 when viewed at an angle. The open arrows show the "steps" of the crack propagation while the solid arrows indicate microcracks in the raceway.

Stress Analysis

An estimate of the stress necessary to propagate a microcrack in this material was made using the following fracture mechanics equation:

$$\sigma = \frac{K_{Ic}}{Y \sqrt{a}}$$

where: σ is the stress at fracture; K_{Ic} is the fracture toughness; Y is the unitless shape factor for the crack and a is a measure of the crack size, in this case the depth.

A stress range of 535 to 586 MPa was calculated based on a toughness of 4.1 MPa*$\sqrt{m}$ (from Table 1), microcrack depths of 25 and 30 µm and Y = 1.4 (for a semielliptical crack at the surface). This stress range falls between the flexure and tensile strength values listed in Table 1, however, it is very close to the biaxial strength value of 500 MPa reported by Quinn and Wirth[15] for NC-132. It appears that biaxial strength data is a better indication of the strength of this material under these specific bearing conditions.

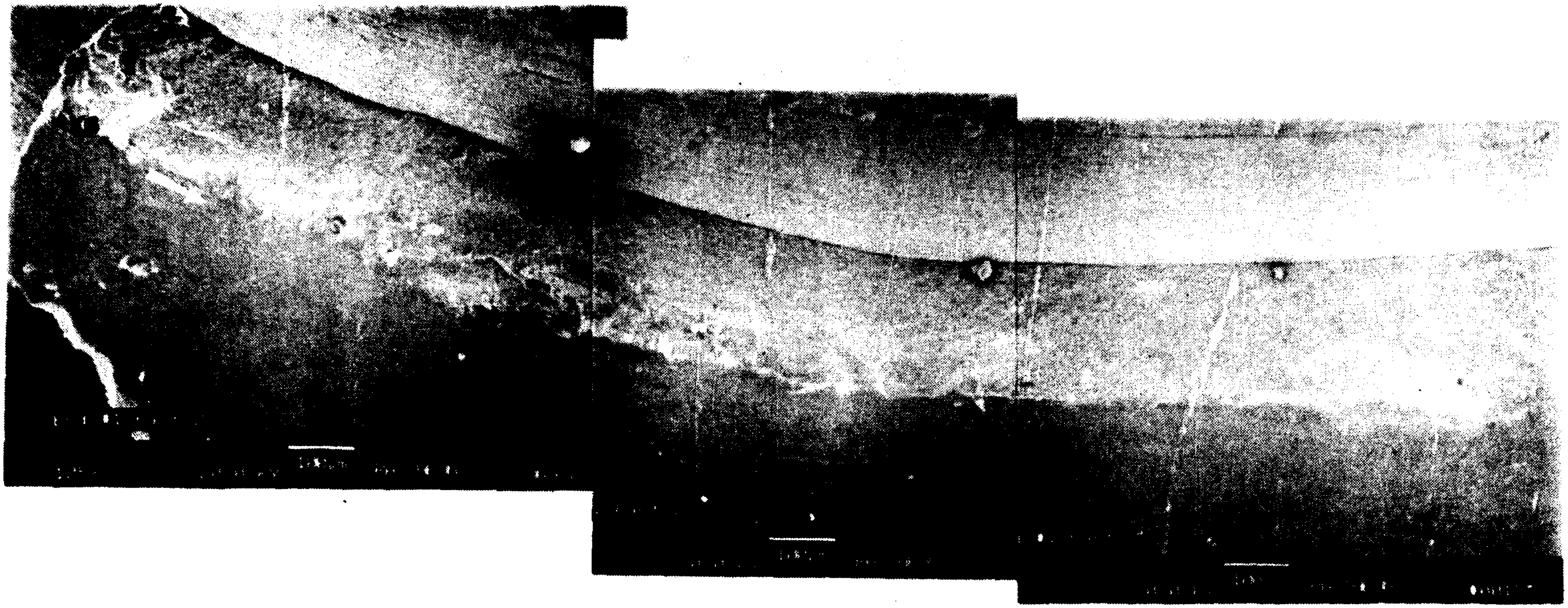

Figure 11. Montage of the fracture surfaces of part 2. X indicates a ball location and the white arrow the direction of crack propagation.

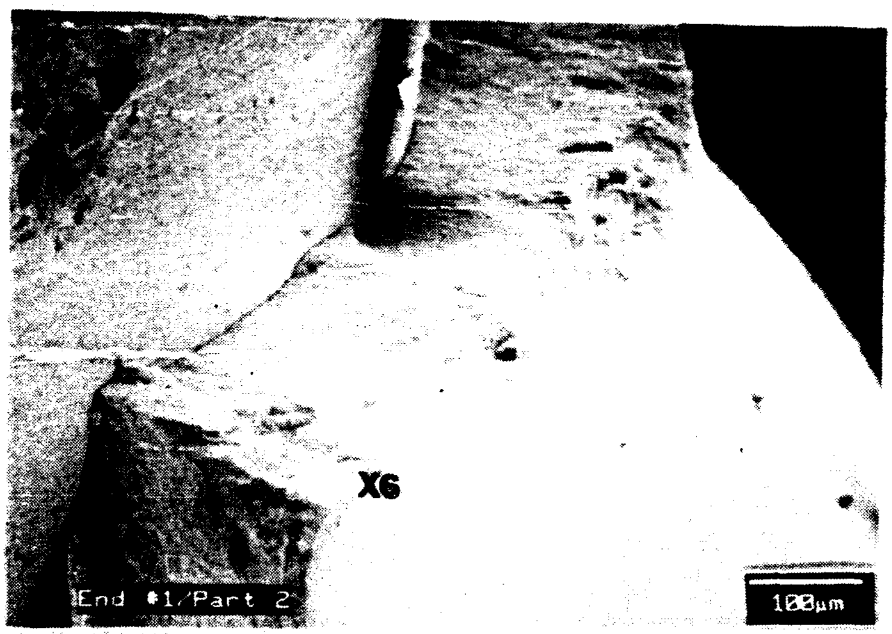

Figure 12. View of part 2 from an angle revealing the rough texture of the fracture surface just below the raceway surface and the smoother texture as the crack proceeds away from the surface. X indicates a ball location and the white arrow the direction of crack propagation.

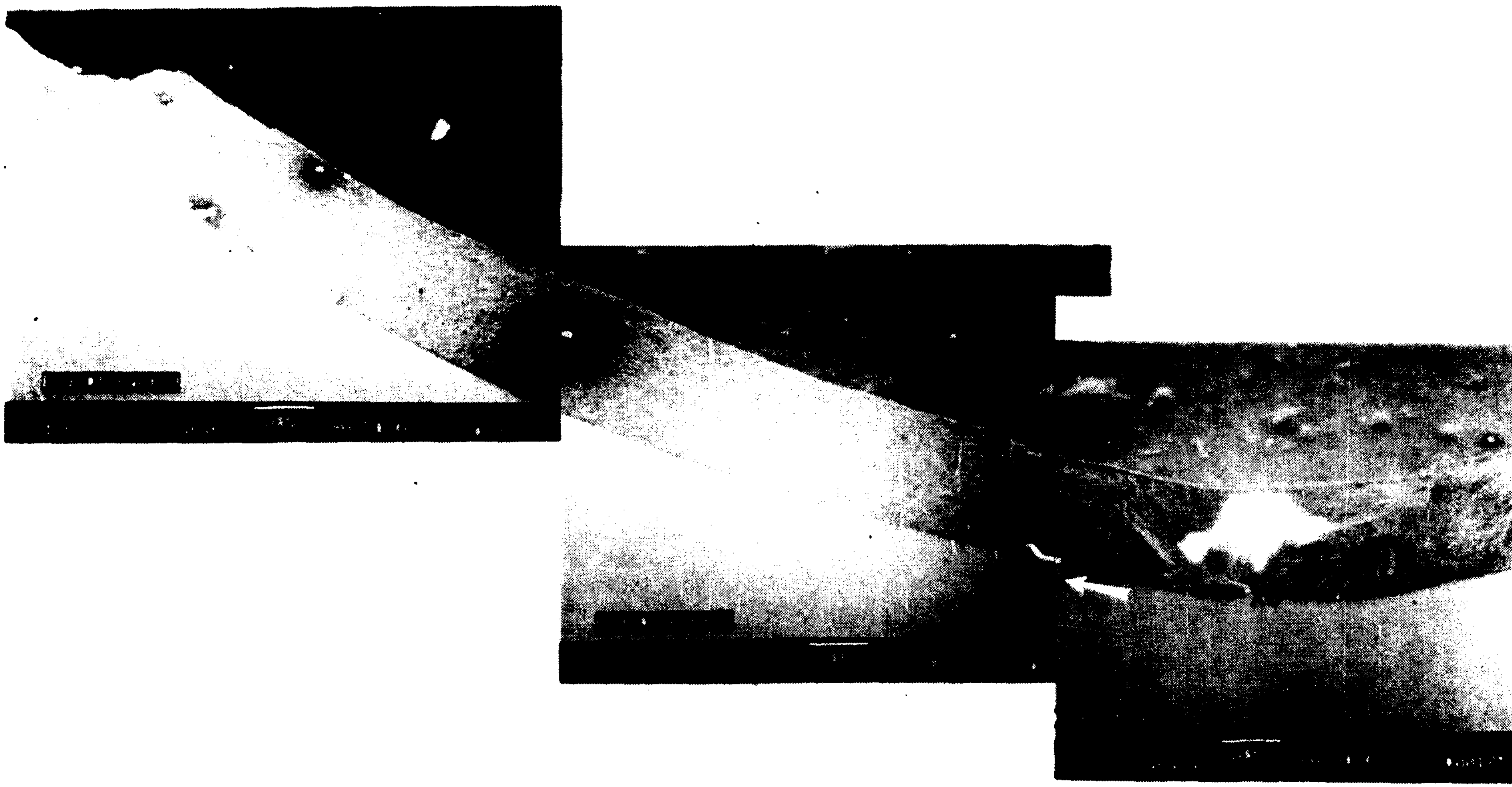

Figure 13. Montage of part 3. Note the change in texture as the crack proceeds between the balls (marked X6) and the end of the part. The white arrow indicates the direction of crack propagation.

DISCUSSION

The fracture analysis of this failed ceramic bearing system raised the following questions which will be answered in this section:

1) Why did the inner races fracture?
2) What caused the macrocracks to initiate?
3) How did microcracks get in to the material?
4) What can be done to reduce or eliminate these microcracks?

1) Why did the inner races fracture? - Based on the fractographic analysis fracture initiated at or very close to a ball location in the raceway of both inner races. Since the balls were held in place during the test the stresses created by a sphere on a plate can be used to describe why the inner races fractured but the outer race did not. When a sphere is compressed onto a plate the forces created in the plate are tensile as well as compressive. The compressive forces are perpendicular to the ball/plate contact area while the tensile forces act radially in this area.

In this bearing system it is assumed that the force of the ball on the outer raceway is the same as that on the inner raceway. This results in a different stress beneath the ball in each raceway due to a difference in the ball/raceway contact area. The contact area of the outer raceway is greater than that of the inner raceway because the direction of the axial and radial curvature of the outer raceway is the same as the ball. Thus the distribution of the tensile stress will approach a circle since the these stresses will be essentially equal in all directions. This is not the case for the inner raceway since the axial curvature of the raceway is in the same direction as the ball but the radial curvature is in the opposite direction. This results in an elliptical stress distribution with the highest tensile stresses aligned in the radial direction.

This not only accounts for why the inner races fractured instead of the outer race, but also explains why the macrocracks traversed the circumference (radial axis) of the inner raceway.

2) What caused the macrocracks to initiate? - The fractographic evidence points to the growth and coalesce of microcracks beneath or very close to a ball/raceway contact area as the beginning of fracture. A series of these microcracks are quite obvious on the fracture surface of part 1, see Figure 9. The rough texture of the fracture surface on the outside edge of the raceway, Figures 11 and 12, and at or very near the location of a ball, Figure 13, also indicates that microcracks were growing. The tensile stresses in the ball/raceway contact area promoted the growth of these microcracks until they coalesce to form the macrocracks which ultimately resulted in fracture.

The growth of microcracks can also account for the variations in the amount of damage at each ball location. First the stress at each ball location may be different, probably less than the stress in area A, which will affect how many and too what extent microcracks will grow. The interaction between the micro- and macrocracks will also influence the amount of damage. As the macrocrack propagates it will encounter the microcracks beneath and around each ball. The energy supplied by the macrocrack will cause many microcracks to grow simultaneously. Thus

the piece missing at each ball location (X1, X2, X5 and X6) is probably not a single piece but rather many pieces that were created due to this interaction. Each interaction will reduce the energy of the macrocrack resulting in less damage at the next ball location. This explains why the damage at X3 and X4 is significantly less than at the other ball locations.

3) How did microcracks get in to the material? - Most ceramic components will require some degree of machining (typically diamond grinding) to produce a finished product. Diamond grinding can introduce microcracks in to the ceramic which adversely affect the performance of the component. In order to minimize this damage a step-wise grinding process is commonly used where in the initial grinding is done with a coarse grit wheel followed by grinding with finer and finer grit wheels. The finer grinding steps attempt to remove any damage done by the coarser grinding steps. Unfortunately the initial coarse grinding steps can produce subsurface microcracks which are not removed during the subsequently finer grinding steps but the evidence that damage was done will be removed. (It should be noted that grinding with fine grit wheels can also cause damage.) Studies by Mecholsky et. al.[16] and Rice, et. al.[17] have shown that grinding can reduce the strength of glasses and polycrystalline ceramics. In bearings Dalal[3] reported that the fatigue life of NC-132 balls will depend on the type of diamond grinding procedure, while Baumgartner[4] found that the growth of microcracks leads to spall formation in NC-132 and in order to increase the life of the bearing the amount of microcracks must be minimized.

The first fractographic indication that the microcracks in this system were related to machining was the appearance (uniform shape and size) of the series of subsurface microcracks in Figure 9. Similar machining induced cracks have been shown to limit the strength of silicon nitride[18] and other ceramic materials.[19] Second was the step-wise propagation of the crack (see Figure 10) in part 1. Mecholsky et. al.[16] showed that grinding introduces two types of microcracks: one which is parallel to the grinding direction and one which is perpendicular to the grinding direction. The parallel microcracks are typically more severe. The grinding direction of the raceways is along the radial axis. Based on the stress state discussed previously the axial tensile stresses appear to be sufficient to grow the parallel (more severe) microcracks while the radial tensile stresses grow the perpendicular microcracks. These growing microcracks then link together, with the parallel microcracks becoming the steps and the perpendicular microcracks the risers, resulting in the step-wise propagation of the crack.

4) What can be done to reduce or eliminate these microcracks? - The most obvious answer is to used an alternate machining process that does not introduce microcracks in to the ceramic. Unfortunately at present, there are no alternatives to diamond grinding of silicon nitride. However, the following recommendations to adjust the machining procedure may be sufficient for this ceramic bearing application.

1) Develop a machining procedure specifically for the raceways.
2) Reduce the material removal rate during coarse grinding.
3) Eliminate grinding with coarse grit wheels.

These recommendations may not be cost-effective or even feasible. Thus an alternative

suggestion would be to subject the NBD-200 material to a post-machining heat treatment. Previous work on NC-132[11,20] has shown that short duration exposures (< 10 hours) at temperatures approaching 1200°C result in an increase in the room temperature strength. This increase is due to the relaxation of the residual stresses created during machining and/or a change in the acuity of the cracks in the material.

CONCLUSION

Machining-related microcracks were shown to limit the load capacity of an all-ceramic bearing system which failed during design load margin testing. The stress imparted on the inner raceway by the ball caused these microcracks to grow. This growth ultimately resulted in the formation of macrocracks which traversed the circumference of the raceway. The effects of these microcracks may be reduced by adjusting the machining parameters or by subjecting the components to a short duration post-machining heat treatment.

ACKNOWLEDGMENT

The authors would like to thank George Gazza and Michael Slavin of the Ceramics Research Branch at Materials Directorate of the U.S. Army Research Laboratory for their fruitful and informative discussions during the course of this analysis.

This work was part of the Advanced Ceramic Technology Insertion program for the Naval Air Warfare Center - China Lake, CA and was sponsored by the Advanced Research Projects Agency.

REFERENCES

1. H.R. Baumgartner, "Evaluation of Roller Bearings Containing Hot-Pressed Silicon Nitride Rolling Elements," Ceramics for High Performance Applications, J.J. Burke, A.E. Gorum, and R.N. Katz, eds., Brook Hill Publishing, Chestnut Hill, MA, 713-727 (1974).

2. D. Steinmann, "Silicon Nitride Ceramics for Balls and Ball Bearings," Ceram. Forum, Int., 67 [12] 584-588 (1990).

3. H. Dalal, "Machining Bearings for Turbine Applications," Ceramics for High Performance Applications - II, J.J. Burke, E.N. Lenoe, and R.N. Katz, eds., Brook Hill Publishing, Chestnut Hill, MA, 407-422 (1978).

4. H.R. Baumgartner, "Ceramic Bearings for Turbine Applications," Ceramics for High Performance Applications - II, J.J. Burke, E.N. Lenoe, and R.N. Katz, eds., Brook Hill Publishing, Chestnut Hill, MA, 423-443 (1978).

5. Y.P. Chiu and H. Dalal, "Lubricant Interaction with Silicon Nitride in Rolling Contact Applications," Ceramics for High Performance Applications, J.J. Burke, A.E. Gorum, and R.N. Katz, eds., Brook Hill Publishing, Chestnut Hill, MA, 589-607 (1974).

6. C.F. Bersch, "Overview of Ceramic Bearing Technology," Ceramics for High Performance Applications - II, J.J. Burke, E.N. Lenoe, and R.N. Katz, eds., Brook Hill Publishing, Chestnut Hill, MA, 397-405 (1978).

7. R.N. Katz and J.G. Hannoosh, "Ceramics for High Performance Rolling Element Bearings: A Review and Assessment," Int. J. High Tech. Ceram., 1, 69-79 (1985).

8. L.B. Sibley, "Silicon Nitride Bearing Elements for High-Speed High-Temperature Applications," Problems in Bearings and Lubrication, AGARD Conference Proceedings No. 323, AGARD, Neuilly sur Seine, France, Chapter 5 (1982).

9. S.W. Freiman, J.J. Mecholsky, W.J. McDonough and R.W. Rice, "Effect of Oxidation on the Room Temperature Strength of Hot-Pressed Si_3N_4-MgO and Si_3N_4-ZrO_2," Ceramics for High Performance Applications - II, J.J. Burke, E.N. Lenoe, and R.N. Katz, eds., Brook Hill Publishing, Chestnut Hill, MA, 1069-1076 (1978).

10. R.K. Govila, "Uniaxial Tensile and Flexure Stress Rupture of Hot Pressed Si_3N_4," J. Am. Ceram. Soc., 65 [1] 15-21 (1982).

11. N. Tighe and S. Wiederhorn, "Effects of Oxidation on the Reliability of Hot Pressed Silicon Nitride," Fracture Mechanics of Ceramics, Vol. 5, R.C. Bradt, A.G. Evans, D.P.H. Hasselman and F.F. Lange, eds., Plenum Press Corp., 403-424 (1983).

12. G.D. Quinn, "Fracture Mechanism Maps for Advanced Structural Ceramics, Part 1: Methodology and Hot-Pressed Silicon Nitride Results," J. Mat. Sci. 25, 4361-4376 (1990).

13. "Corrosion in the Aircraft Industry," Corrosion: Metals Handbook, 9th Edition, Volume 13, 1018-1057, ASM International, Metals Park, OH (1987).

14. B. O'Dwyer, "Gimbal Bearing," U.S. Patent #5,215,386, awarded 1 June 1993.

15. G. Quinn and G. Wirth, "Biaxial Stress Rupture of Silicon Nitride," Mat. Sci. Eng., A109, 147-152 (1989).

16. J.J. Mecholsky, Jr., S.W. Freiman and R.W. Rice, "Effect of Grinding on Flaw Geometry and Fracture of Glass," J. Am. Ceram. Soc., 60 [3-4] 114-117 (1977).

17. R.W. Rice, J.J. Mecholsky, Jr. and P.F. Becher, "The Effect of Grinding Direction on Origin Character and Strength of Single Crystal and Polycrystalline Ceramics," J. Mat. Sci., 16, 853-862 (1981).

18. V.K. Pujari, D.M. Tracey, M.R. Foley, N.I. Paille, P.J. Pelletier, L.C. Sales, C.A. Wilkens and R.L Yeckley, "Development of Improved Processing and Evaluation Methods for High Reliability Structural Ceramics for Advanced Heat Engine Applications, Phase I," Oak Ridge National Laboratory, ORNL/Sub/89-SB182/1, August 1993.

19. J.J. Swab and S.C. Stowell, "Properties of a TZP/Al_2O_3 Composite After Long-Term Exposure at 1000°C," U.S. Army Materials Technology Laboratory, MTL TR 91-54, December 1991, NTIS Access No. ADA-2464407.

20. F.F. Lange, B.I. Davis and M.G. Metcalf, "Strengthening of Polyphase Si_3N_4 Materials Through Oxidation," J. Mat. Sci., 18 1497-1505 (1983).

DISTRIBUTION LIST

No. of Copies	To
1	Office of the Under Secretary of Defense for Research and Engineering, The Pentagon, Washington, DC 20301
	Director, U.S. Army Research Laboratory, 2800 Powder Mill Road, Adelphi, MD 20783-1197
1	ATTN: AMSRL-OP-SD-TP, Technical Publishing Branch
1	AMSRL-OP-SD-TA, Records Management
1	AMSRL-OP-SD-TL, Technical Library
	Commander, Defense Technical Information Center, Cameron Station, Building 5, 5010 Duke Street, Alexandria, VA 23304-6145
2	ATTN: DTIC-FDAC
1	MIA/CINDAS, Purdue University, 2595 Yeager Road, West Lafayette, IN 47905
	Commander, Army Research Office, P.O. Box 12211, Research Triangle Park, NC 27709-2211
1	ATTN: Information Processing Office
	Commander, U.S. Army Materiel Command, 5001 Eisenhower Avenue, Alexandria, VA 22333
1	ATTN: AMCSCI
	Commander, U.S. Army Materiel Systems Analysis Activity, Aberdeen Proving Ground, MD 21005
1	ATTN: AMXSY-MP, H. Cohen
	Commander, U.S. Army Missile Command, Redstone Arsenal, AL 35809
1	ATTN: AMSMI-RD-CS-R/Doc
	Commander, U.S. Army Armament, Munitions and Chemical Command, Dover, NJ 07801
1	ATTN: Technical Library
	Commander, U.S. Army Natick Research, Development and Engineering Center Natick, MA 01760-5010
1	ATTN: SATNC-MI, Technical Library
	Commasnder, U.S. Army Satellite Communications Agency, Fort Monmouth, NJ 07703
1	ATTN: Technical Document Center
	Commander, U.S. Army Tank-Automotive Command, Warren, MI 48397-5000
1	ATTN: AMSTA-ZSK
1	AMSTA-TSL, Technical Library
	President, Airborne, Electronics and Special Warfare Board, Fort Bragg, NC 28307
1	ATTN: Library
	Director, U.S. Army Research Laboratory, Weapons Technology, Aberdeen Proving Ground, MD 21005-5066
1	ATTN: AMSRL-WT

No. of Copies	To
	Commander, Dugway Proving Ground, UT 84022
1	ATTN: Technical Library, Technical Information Division
	Commander, U.S. Army Research Laboratory, 2800 Powder Mill Road, Adelphi, MD 20783
1	ATTN: AMSRL-SS
	Director, Benet Weapons Laboratory, LCWSL, USA AMCCOM, Watervliet, NY 12189
1	ATTN: AMSMC-LCB-TL
1	AMSMC-LCB-R
1	AMSMC-LCB-RM
1	AMSMC-LCB-RP
	Commander, U.S. Army Foreign Science and Technology Center, 220 7th Street, N.E., Charlottesville, VA 22901-5396
3	ATTN: AIFRTC, Applied Technologies Branch, Gerald Schlesinger
	Commander, U.S. Army Aeromedical Research Unit, P.O. Box 577, Fort Rucker, AL 36360
1	ATTN: Technical Library
	U.S. Army Aviation Training Library, Fort Rucker, AL 36360
1	ATTN: Building 5906-5907
	Commander, U.S. Army Agency for Aviation Safety, Fort Rucker, AL 3636
1	ATTN: Technical Library
	Commander, Clarke Engineer School Library, 3202 Nebraska Ave., N., Fort Leonard Wood, MO 65473-5000
1	ATTN: Library
	Commander, U.S. Army Engineer Waterways Experiment Station, P.O. Box 631, Vicksburg, MS 39180
1	ATTN: Research Center Library
	Commandant, U.S. Army Quartermaster School, Fort Lee, VA 23801
1	ATTN: Quartermaster School Library
	Naval Research Laboratory, Washington, DC 20375
1	ATTN: Code 6384
	Chief of Naval Research, Arlington, VA 22217
1	ATTN: Code 471
	Commander, U.S. Air Force Wright Research and Development Center, Wright-Patterson Air Force Base, OH 45433-6523
1	ATTN: WRDC/MLLP, M. Forney, Jr.
1	WRDC/MLBC, Mr. Stanley Schulman
	U.S. Department of Commerce, National Institute of Standards and Technology, Gaithersburg, MD 20899
1	ATTN: Stephen M Hsu, Chief, Ceramics Division, Institute for Materials Science and Engineering

No. of Copies	To
1	Committee on Marine Structures, Marine Board, National Research Council, 2101 Constitution Avenue, N.W., Washington, DC 20418
1	Materials Sciences Corporation, Suite 250, 500 Office Center Drive, Fort Washington, PA 19034
1	Charles Stark Draper Laboratory, 555 Technology Square, Cambridge, MA 02139
	Wyman-Gordon Company, Worcester, MA 01601
1	ATTN: Technical Library
	General Dynamics, Convair Aerospace Division, P.O. Box 748, Fort Worth, TX 76101
1	ATTN: Mfg. Engineering Technical Library
	Plastics Technical Evaluation Center, PLASTEC, ARDEC, Bldg. 355N, Picatinny Arsenal, NJ 07806-5000
1	ATTN: Harry Pebly
1	Department of the Army, Aerostructures Directorate, MS-266, U.S. Army Aviation R&T Activity - AVSCOM, Langley Research Center, Hampton, VA 23665-5225
1	NASA - Langley Research Center, Hampton, VA 23665-5255
	U.S. Army Vehicle Propulsion Directorate, NASA Lewis Research Center, 2100 Brookpark Road, Cleveland, OH 44135-3191
1	ATTN: AMSRL-VP
	Director, Defense Intelligence Agency, Washington, DC 20340-6053
1	ATTN: ODT-5A, Mr. Frank Jaeger
	U.S. Army Communications and Electronics Command, Fort Monmouth, NJ 07703
1	ATTN: Technical Library
	U.S. Army Research Laboratory, Electronic Power Sources Directorate, Fort Monmouth, NJ 07703
1	ATTN: Technical Library
1	Jeff Abboud, U.S. Advanced Ceramics Assn., 1600 Wilson Boulevard, Suite 1008, Arlington, VA 22209
1	Dr. James Adair, University of Florida, Department of Materials Science and Engineering, 217 MAE, Gainesville, FL 32611-2066
1	Oyelayoo O. Ajayi, Wedeven Associates, Inc., 5072 West Chester Pike, Edgemont, PA 19028
1	David Arwell, General Dynamics EB Division, 75 Eastern Point Road, Groton, CT 06340

No. of Copies	To
1	Manohar Bashyam, GE Aircraft Engines, 10270 St. Rita Lane, Q 45, Cincinnati, OH 45215
1	John C. Bennett, MRC Bearings, Rt. 8, 149 Colebrook Road River, Winsted, CT 06098
1	Joe Bentz, Enceratec, 810 Brown Street, Columbus, OH 47201
1	Charles F. Bersch, IDA, 1801 N. Beauregard Street, Alexandria, VA 22311
1	Dr. Vivek Bhargave, GE - Corp. R&D, P.O. Box 8, Bldg. K1, 4B4, Schenectady, NY 12301
1	James Bird, Amersom, 8928 Fullbright Avenue, Chatsworth, CA 91311
1	Hugh Blackwell, PSD 312, Navavn Depot, MSAS, Cherry Point, NC 28533
1	Eric Blumer, Allied Signal Engines, P.O. Box 52181, Phoenix, AZ 85072-2181
1	David Born, The Dow Chemical Company, 800 Building, Midland, MI 48667
3	Duncan Boyce, Raytheon, 50 Apple Hill Drive, Tewksbury, MA 01876
1	David Brown, NASA, EH13, Huntsville, AL 35812
1	Wade Brown, Kaiser Aerotech, 880 Doolittle Drive, San Leandro, CA 94577
1	Otto Buck, DOE/BES Materials Science Division, ER-131 GTN, Washington, DC 20585
1	Lyman Burgmeier, Allied Signal, 2525 W. 190th Strees, Torrance, CA 90504-6099
1	Charles Burk, Cerbec, 10 Airport Park Road, East Granby, CT 06026
1	Harold Burrier, Jr. - RES09, The Timken Co., P.O. Box 6930, 1835 Dueber S.W., Canton, OH 44706-0903
1	Dave Carruthers, Kyocera Industrial Ceramics, 1513 E. Fourth Plain Boulevard, Vancouver, WA 98661
1	Ming Chen, WL/MLBM Surface/Interactions, 2941 P. Street, Suite 1, WPAFB, OH 45433-775
	The Torrington Company, 59 Field Street, Torrington, CT 06790-4942
1	ATTN: Y. P. Chiu
1	William Chmura
1	Michael M. Dezzani
1	Leon Chuck, University of Dayton, 300 College Park, KL-165, Dayton, OH 45469-0172
	Pratt & Whitney - GESP, P.O. Box 109600, West Palm Beach, FL 33410-9600
1	ATTN: Kenneth Clodfelter
1	Chris Farral
1	Dr. William S. Coblenz, ARPA/DSO, 3701 N. Fairfax Drive, Arlington, VA 22203-1714

No. of Copies	To
1	Bill Crecelius, GE Aircraft Engines, One Neuman Way, Cincinnati, OH 45215
	Mechanical Technology, Inc., 968 Albany - Shaker Road, Latham, NY 12110
1	ATTN: Michael J. Cronin
1	Dr. James Dill
1	Raymond Cutler, Ceramatec, Inc., 2425 So. 900 W., Salt Lake City, UT 84119
1	Jonathan Dell, WL/POSL Bldg. 490, 1790 Loop Road N., APAFB, OH 45433-7103
1	Stephen Didziulis, The Aerospace Corporation, P.O. Box 92957, MS M2-271, Los Angeles, CA 90009-2957
1	Allison Gas Turbine Division, GM, P.O. Box 420, Speed Code U01A, Indianapolis, IN 46206-0402
1	ATTN: Julie J. Dornfled
1	Michael Dowell, Advanced Ceramics Corp., P.O. Box 94924, Cleveland, OH 94924
1	Michael Drory, Crystallume, 125 Constitution Drive, Menlo Park, CA 94025
1	Bill Durako, Sundstrand Aerospace, P.O. Box 7002, Mail Stop 741A6, Rockford, IL 61125-7002
1	George Dvorak, Rensselaer Polytechnic Institute, Department of Civil & Environmental Engineering, Troy, NY 12180-3590
1	Franz-Josef Ebert, F.A.G. Bearings, LTD., 801 Ontario Street, Stratford, Ontario N5A 6T2
1	Dr. William Ellingson, Argonne National Lab., 9700 S. Cass Avenue, Argonne, IL 60439
1	Dr. Stanley H. Evans, Jr., Alpha Optical Systems, Inc., 1611 Government Street, Ocean Springs, MS 39564
1	Andre Ezis, Cercom, Inc., 1960 Watson Way, Vista, CA 92083
1	Robert Feest, Barden Corporation, 200 Park Avenue, Danbury, CT 06813
1	Traugott Fischer, Steven I.T., Hoboken, NJ 07030
1	Hans Frederícy, Allied Signal Aerospace, 1530 Wilson Boulevard, Suite 1000, Arlington, VA 22209
1	Anthony T. Galbato, MRC Bearings, 401 Chandler Street, Jamestown, NY 14701
1	Dr. Michael N. Gardos, Hughes Aircraft Company, P.O. Box 902, E1/F150, El Segundo, CA 90245

No. of Copies	To
1	Dr. John E. Garnier, DuPont Lanxide Composites, P.O. Box 6077, 1 Tralee Industrial Park, Newark, DE 19714-6077
1	Dr. Richard S. Gates, NIST, Building 223, Room A256, Gaithersburg, MD 20899
1	Peter Gaydos, Battelle, 505 King Avenue, Columbus, OH 43201
1	Keith Gordon, MPB, P.O. Box 547, Keene, NH 03431
1	Lance Groseclose, Allison Gas Turbine, P.O. Box 420, Indianapolis, IN 46206
1	Dr. Pradeep Gupta, PKG, Inc., 117 Southbury Road, Clifton Park, NY 12065
1	Mr. Joseph Halada, DuPont Lanxide Composites, P.O. Box 6077, 1 Tralee Industrial Park, Newark, DE 19714-6077
1	Bob Hardesty, Spheric, Inc., 9450 7th Street, Suite 1, Bldg. 655 WL/MLLM, WPAFB, OH 45433-7817
1	Susan Hastings, WL Materials Directorate, 2230 Tenth Street, Suite 1, Bldg. 655 WL/MLLM, WPAFB, OH 45433-7817
1	Michael R. Hoeprich, The Timken Company, 1835 Dueber Avenue, P.O. Box 6930, Canton, OH 44706-0930
1	William Hong, Institute for Defense Analyses, 1801 N. Beauregard Street, Alexandria, VA 22311
1	John E. Holowczak, United Technologies, Research Center, Engineered Ceramics Group, 411 Silver Lane, MS 129-22, E. Hartford, CT 06108
1	Richard Houghton, MPB Corporation, P.O. Box 547, Keen, NH 03431
1	Roy B. Howarth, Mechanical Technology Inc., 968 Albany-Shaker Road, Latham, NY 12110
1	Dr. Stephen Hsu, NIST, Room A-263, Building 223, Gaithersburg, MD 20899
1	Pat Hughes, Commander Navy Sea Systems Command, Code NAVSEA 08T, 2531 Jefferson Davis Highway, Arlington, VA 22242-5160
1	Said Jahanamir, NIST, Room A329, Building 223, Gaithersburg, MD 20899
1	Stephen R. Johnson, GE Aircraft Engines, One Neuman Way, M/D A328, Cincinnati, OH 45215-6301
1	Ronald V. Kadyszewski, Vickers, Inc. - Tedeco DIC, 24 E. Glenolden Avenue, Glenolden, PA 19036
1	Tony Kaushal, Detroit Diesel Corporation, 13400 Outer Drive West, Detroit, MI 48239-4001

No. of Copies	To
1	Mike Keelan, Detroit Diesel Corporation, 13400 Outer Drive West, Detroit, MI 48239-4001
1	William Kelleher, Draper Labs, 555 Tech Square, Cambridge, MA 02139
1	Ronald Kelley, Strategic Partners, Inc., 1025 Thomas Jefferson Street, NW, Washington, DC 20007
6	Rod B. Kenly, Naval Air Warfare Center, C29B3, China Lake, CA 93555-6001
1	Ranga Komanduri, Oklahoma State University, Mechanical Engineering Department, Stillwater, OK 74078
1	Paul M. Komater, Pratt & Whitney, MS 706-38, P.O. Box 109600, West Palm Beach, FL 33410-9600
1	James Lange, Oklamoma State University, 145 Physical Sciences, Stillwater, OK 74078
1	Thomas Leo, Cerbec, Inc., 10 Airport Park Road, East Granby, CT 06026
1	Stanley R. Levine, NASA Lewis Research Center, 21000 Brookpark Road, MS 106-5, Cleveland, OH 44135
1	Bill Long, Babcock & Wilcox, Lynchburg, VA 24506
1	Michael J. Lubas, P.E., General Synamics/Electro Dynamic, 150 Avenel Street, Avenel, NJ 07001
1	Mitchell Machelsi, Thomson Saginaw, Ball Scres Company, 628 N. Hamilton Street, Saginaw, MI 48602
1	Susan Mackie, Department of Defense, 1629 Columbia Road, NW #511, Washington, DC 20009
1	Bill Mandler, Enceratec, 810 Brown Street, Columbus, IN 47201
1	John Mangells, Ceradyne, Inc., 3169 Redhill, Costa Mesa, CA 92629
1	Pete Marrero, SFAE-ASM-AB, Warren, MI 48397-5000
1	Keneth Marnoch, Amercom, 8928 Fullbright Avenue, Chatsworth, CA 91311
1	Dr. Fred Mazandarany, GE Corporation - Research and Development, P.O. Box 8, K1, MB-159, Schnectady, NY 12301
1	Bobby McConnell, Tribotech Consultants, 43 Monterey Road, Dayton, OH 45419-2566
1	Dr. J. J. Mecholsky, University of Florida, Department of Materials Science and Engineering, 256A Rhines Hall, Gainesville, FL 32611-2066
1	John Miner, United Technologies, Pratt & Whitney - GESP, P.O. Box 109600, West Palm Beach, FL 33410

No. of Copies	To
1	Karl R. Mecklenburg, WL/MLBT, Bldg. 654, 2941 P Street, Suite 1, WPAFB, OH 45433-7750
1	Crawford R. Meeks, AVCON, 5210 Lewis Road, Agoura Hills, CA 91301
1	Dr. Peter E. D. Morgan, Rockwel International Science, 1049 Camino Dos Rios, Thousand Oaks, CA 91360
1	Jim Mosquera, Commander, Navy Sea Systems, Command, Code NAVSEA 08T, 2531 Jefferson Davis Highway, Arlington, VA 22242-5160
1	Tom Myers, OC-ALC, 3001 Staff Drive, Suite 1AC196H, Tinker Air Force Base, OK 73145-3029
1	John O'Donnell, NAWCAD Trenton, P.O. Box 7176, Code PE32, Trenton, NJ 08628-0176
1	Reed R. Oliver, GE Aircraft Engines, M.D. G52 One Neuman Way, Evendale, OH 45215
1	David Paaavola, Winsted Precision Ball Company, 248 Rockwell Street, Winsted, CT 06098
1	Phil Pearson, The Torrington Company, 59 Field Street, Torrington, CT 06790
1	Eugene Pfaffenberger, Allison Gas Turbine Division - GM, 2001 S. Tibbs Avenue, Indianapolis, IN 46206-0420
1	Joe Poplawski, J. V. Poplawski & Associates, 1480 Valley Center Parkway, Bethlehem, PA 18017
1	Matt Poursaba, OC-ALC/LIIRE, 3001 Staff Drive, Suite 1AC196H, Tinker Air Force Base, OH 73145-3029
1	Robert Price, Draper Labs, 555 Tech Square, Cambridge, MA 02139
1	Dr. William Rafaniello, The Dow Chemical Company, Bldg. 1776, Midland, MI 48674
1	Mark Rhoads, GE Aircraft Engines, One Neuman Way, MD M85, Cincinnati, OH 45215-6301
1	Dr. George W. Rhodes, Quatro Corporation, 4300 San Mateo Boulevard, Albuquerque, NM 87710
1	Jon Salem, NASA LERC, 21000 Brookpark Road, Cleveland, OH 44135
1	Clifford A. Schaefer, SA-ALC/LDPE, 485 Quentin Roosevelt Road, Kelly Air Force Base, TX 78241-6426
1	Thomas R. Schneider, Hohman Plating & Manufacturing, Inc., 814 Hillrose Avenue, Dayton, OH 45404
1	Neil Seelen, Hoover Precision Products, 35 Kripes Road, East Granby, CT 06026
1	Dinesh K. Shetty, University of Utah, 304 EMRO, Salt Lake City, UT 84112

No. of Copies	To
1	James Shih, Cercon, Inc., 1960 Watson Way, Vista, CA 92083
1	Lew Sibley, Tribology Systems, Inc., 225A Plank Avenue, Paoli, PA 19301-1726
1	Hans R. Signer, Industrial Tectonics Brgs Company, 18301 Sante Fe Avenue, Rancho Dominguez, CA 90224
1	Dennis Smith, Honeywell, Satellite Systems, P.O. Box 52199, Phoenix, AZ 85072-2199
1	Jay R. Smyth, ALlied Signal Aerospace, 93-173/1303-207, 2739 E. Washington Street, P.O. Box 52180, Phoenix, AZ 85072-2180
1	William D. Sproul, Birl, Northwestern University, 1801 Maple Avenue, Evanston, IL 60201
1	P. Richard Stoesser, The Dow Chemical Company, Bldg. 1776, Midland, MI 48674
1	Tatiana Strainic, U.S. Advanced Ceramics Association, 1600 Wilson Boulevard, Suite 1008, Arlington, VA 22209
1	Bernard C. Stupp, Homan Plating & Manufacturing, Inc., 814 Hillrose Avenue, Dayton, OH 45404
1	Ed Taschner, 74-59/2102-404, Allied Signal Engines, 1944 E. Sky Harbor Circle, Phoenix, AZ 85038
1	Bruce Thomson, Textron Specialty Materials, 2 Industrial Avenue, Lowel, MA 01851
1	AHN Tran, Aerospace Corporation, 2350 E. El Segundo Boulevard, El Segundo, CA 90245
1	Long Tran, AVCON, 5210 Lewis Road, Suite 14, Agoura Hills, CA 91301
1	Archie R. Tyrone, SA-ALC/LDPG, 485 Quentin Roosevelt Road, Kelly Air Force Base, OH 78241-6426
1	Dr. Kathryn Wahl, Naval Research Laboratory, Code 6176, Washington, DC 20375-5320
1	Ron Walecki, Ceramic Components, 2525 W. 190th Street, Torrance, CA 90504
1	Shenandoah Wang, Industrial Tectonics Brgs., 18301 S. Santa Fe Avenue, Rancho Dominguez, CA 92067
1	Shaio-Wen Wang, Naval Air Warfare Center, Aircraft Division, Warminster, Code G064, Street Road, Warminster, PA 18974
1	Mark Warburton, General Dynamics EB Division, 75 Eastern Point Road, Groton, CT 06340
1	Dr. Christian Weber, University of California Santa Barbara, Materials Department, Santa Barbara, CA 93106
1	James Wessel, Dow Corning Corporation, 1800 M Street, N>W>, #325 South, Washington, DC 20036

No. of Copies	To
1	Dr. Albert Wey, Sonoscan, Inc., 530 Green Street, Bensenville, IL 60106
1	Ben Wilcox, ARPA, Materials Science Division, 37001 N. Fairfax Drive, Arlington, VA 22203-1714
1	Adrian Wood, MPB Corporation, P.O. Box 547, Precision Park, Keene, NH 03431
1	George Quinn, Ceramics Division, National Institute of Standards and Technology, Gaithersburg, MD 20899
	Raytheon Company, Missile Systems Laboratories, 50 Apple Hill Drive, Tewksbury, MA 01876
6	ATTN: Mary Sweeney, Mail Stop T3LC21
1	Andrew Goldman, Mail Stop T3LE03
1	Robert Eckel, Mail Stop T3LC21
1	Robert McCombs, Mail Stop T3SP33
1	Thomas Briere, Mai Stop T3LC21
1	Diane Dockham, Mail Stop T1LA10
1	David Martin, Mail Stop T3TL10
1	Don LaLiberte, Mail Stop T3TL10
1	Peter Boland, Mail Stop T1LA10
1	Michelle Gauthier, Mail Stop T3SQ16
1	Charles Fairman, Mail Stop T3SR02
1	Edward Holmes, Mail Stop T3SP33
	Naval Air Warfare Center, China Lake, CA 93555-6001
1	ATTN: Murlyn McGowen, 472G20D
1	Karen Stiff, 472G20D
1	Kathy Smith, 332300D
1	Dr. Dan Harris, 474220D
	MPB, Precision Park, P.O. Box 547, Keene, NH 03143-0547
1	ATTN: David R. Breton
1	Sid O. Davis
1	Edward R. Schillemat, Jr.
1	Barry O'Dwyer
	Director, U.S. Army Research Laboratory, Watertown, MA 02172-0001
2	ATTN: AMSRL-OP-WT-IS, Technical Library
10	Authors